Anal Bioanal Chem
DOI 10.1007/s00216-017-0623-0

RESEARCH PAPER

Signal-on electrochemical assay for label-free detection of TdT and BamHI activity based on grown DNA nanowire-templated copper nanoclusters

Yufang Hu[1,2] · Qingqing Zhang[1] · Lihua Xu[1] · Jiao Wang[1] · Jiajia Rao[1] · Zhiyong Guo[1] · Sui Wang[1]

Received: 12 June 2017 / Revised: 31 August 2017 / Accepted: 4 September 2017

Abstract Electrochemical methods allow fast and inexpensive analysis of enzymatic activity. Here, a simple and yet efficient "signal-on" electrochemical assay for sensitive, label-free detection of DNA-related enzyme activity was established on the basis of terminal deoxynucleotidyl transferase (TdT)-mediated extension strategy. TdT, which is a template-independent DNA polymerase, can catalyze the sequential addition of deoxythymidine triphosphate (dTTP) at the 3'-OH terminus of single-stranded DNA (ssDNA); then, the TdT-yield T-rich DNA nanowires can be employed as the synthetic template of copper nanoclusters (CuNCs). Grown DNA nanowires-templated CuNCs (noted as DNA-CuNCs) were attached onto graphene oxide (GO) surface and exhibited unique electrocatalytic activity to H_2O_2 reduction. Under optimal conditions, the proposed biosensor was utilized for quantitatively monitoring TdT activity, with the observed LOD of 0.1 U/mL. It also displayed high selectivity to TdT with excellent stability, and offered a facile, convenient electrochemical method for TdT-relevant inhibitors screening. Moreover, the proposed sensor was successfully used for BamHI activity detection, in which a new 3′-OH terminal was exposed by the digestion of a phosphate group. Ultimately, it has good prospects in DNA-related enzyme-based biochemical studies, disease diagnosis, and drug discovery.

Keywords Electrochemical biosensor · Terminal deoxynucleotidyl transferase · BamHI · Copper nanoclusters · Graphene oxide

Introduction

Genetic information is duplicated to produce two alike copies of an organism's genome, and this typical process is addressed as "DNA replication" [1], involving a set of different proteins working methodically [2, 3]. However, there are two main types of enzymes in DNA replication: polymerases and endonucleases. It has been clinically proven that altered expression level and activity of these two enzymes play a critical role in cancer development, and might also deteriorate even further the response to anticancer chemotherapy [4–7]. Hence, the development of effective, sensitive methods for the activity detection of these DNA-related enzymes is of great significance.

As is known, most DNA polymerases implement this reaction effectively by exploiting a DNA or RNA template to direct each incorporation event. This template-dependent polymerization reaction leads to a generated DNA chain that is complementary to the template strand on the basis of proper Watson-Crick nucleotide base pairing rules. Nevertheless, one unique polymerase, denoted as terminal deoxynucleotidyl transferase (TdT), executes DNA synthesis without a template [8, 9]. The biological function of TdT is to add random dNTP at 3′-OH terminal DNA during V(D)J recombination, which is the unique mechanism of genetic recombination that occurs only in developing lymphocytes during the early stages of T and B cell maturation [10–12]. TdT also plays a notable role in

Electronic supplementary material The online version of this article (https://doi.org/10.1007/s00216-017-0623-0) contains supplementary material, which is available to authorized users.

✉ Yufang Hu
huyufang@nbu.edu.cn

[1] Faculty of Materials Science and Chemical Engineering, Ningbo University, Ningbo, Zhèjiāng 315211, China

[2] State Key Laboratory of Chemo/Biosensing and Chemometrics, College of Chemistry and Chemical Engineering, Hunan University, Changsha, Hunan 410082, China

Published online: 29 September 2017

cancer as it is overexpressed in acute lymphocytic leukemia (ALL) and acute myelocytic leukemia (AML) [13, 14]. Furthermore, higher levels of TdT activity associate with a poor prognosis as lower remission rates, which is observed in patients with TdT-positive leukemia (36%) relative to patients with normal TdT levels (61%) [15]. Finally, ALL is the most common form of childhood cancer in the United States, presenting with approximately 5000 new cases each year [16]. If left untreated, ALL typically causes death within a few months [17]. Hence, probing TdT activity is significant for cancer-related fundamental biochemical research and pharmaceutical development. Previously, detection of TdT activity was largely focused on immunoassay, biochemical assay, gel electrophoresis, and fluorescent methods [13, 18–22], but some unresolved obstacles still remain, including limited sensitivity, complicated equipment, and a relatively expensive and time-consuming detection procedure. To circumvent these problems, electrochemical method is particularly popular owing to its remarkable features of simple, portable, and inexpensive instrumentation, high sensitivity and selectivity, fast response, as well as low fabrication cost [23]. However, reported electrochemical TdT-relevant biosensors are still rare. Hence, it still remains a challenge to develop a facile, sensitive, and cost-effective electrochemical method for probing the activity of TdT.

Nucleases, including exonucleases and restriction endonucleases, have fundamental significance in cellular events and physiological processes, such as recombination, repair, and analysis of DNA [24, 25]. Thus, endonucleases, which are realized as a "molecular scalpel" with highly specific activity of cleaving DNA [26], have been extensively used in PCR assays, medicinal chemistry, gene mapping, and nanostructures/nanodevices fabrication [27, 28]. Endonucleases in prokaryotic organisms play the role of a defensive system with the principal function of protecting the host genome against foreign DNA, and they have been regarded as important targets in the discoveries of antimicrobial and antiviral drugs [29]. BamHI endonuclease is a site-specific endonuclease and can be employed to detect the hepatitis C virus, demonstrating the biological significance of BamHI [30]. So, exploring BamHI activity has attracted a great deal of attention. Recently, some fluorescence methods were reported for the detection of BamHI activity [21, 31]. However, other analytical techniques, such as electrochemistry, are seldom implicated in BamHI assays, presenting a large unexplored field to investigate.

Metal nanoclusters (MNCs) consist of few atoms, with a core size in the sub-nanometer regime, providing the missing link between atomic and nanoparticle behavior in metals [32, 33]. Their sizes are comparable to the Fermi wavelength of electrons, bringing about molecule-like properties, including size-dependent fluorescence and discrete electronic states [34]. Exploiting these unique properties has resulted in many important and exciting findings of MNCs. Since then, MNCs have drawn considerable research interest in recent years and are widely applied in electronic devices, catalysis, biological imaging, and chemical sensors owing to their unique electrical, physical, and optical properties [35–37]. So far great effort has been directed to noble metal nanoclusters (mainly Au and Ag) due to their facile synthetic procedure and chemical stability [38–40]. However, very promising copper nanoclusters (CuNCs) have received much less attention. Actually, compared to Au and Ag, Cu is significantly less expensive and widely used due to its high conductivity. Furthermore, the synthesis precursors for the preparation of CuNCs are relatively abundant, inexpensive, and readily available from commercial sources; therefore, CuNCs are more favorable for various applications than Au or Ag nanoclusters [41]. Among synthesis methods of CuNCs, DNA-templated CuNCs are becoming increasingly prevalent owing to their fast and easy synthesis, low toxicity, and good biocompatibility. They can be divided roughly into two main classes: random double-stranded DNA-templated CuNCs (dsDNA-CuNCs) and single-stranded poly-T-templated CuNCs (poly-T-CuNCs), but the latter is easier and simpler to synthesize than the former. Generally, this poly-T-CuNCs is strictly length-dependent; only poly-T DNA of length greater than 15 bases can promote formation of CuNCs. Wang and colleagues developed a turn-off nuclease assay and relevant inhibitor screening, which was the first example of the application of poly-T-CuNCs [42]. These length-dependent DNA-CuNCs cause us to ask: Could a long randomly arrayed poly-T sequence be obtained by some particular enzyme, and then could the long poly-T-CuNCs serve as electrochemical biosensing probe for DNA-related enzyme activity detection? The obstacle to test this idea is how to prepare a randomly synthesized T-rich DNA sequence-templated poly-T-CuNCs in a facile way and achieve the electrochemical response of DNA-related enzyme activity. Consequently, the application of the long poly-T-CuNCs in enzyme inspection, particularly in a rapid, simple electrochemical assay of DNA-related enzyme activity, will arouse considerable interest.

In the present work, we established a novel electrochemical method for label-free detection of DNA-related enzyme (such as TdT and BamHI) activity based on the unique electrocatalytic activity of the TdT-related grown DNA nanowires-templated CuNCs (noted as DNA-CuNCs in our work) loaded on the graphene oxide (GO)-modified electrode. TdT, the exceptive polymerase of cancer related-disease, can catalyze the addition of deoxythymidine triphosphate (dTTP) to the 3′-OH terminus of single-stranded DNA (ssDNA). It provides a facile and cost-efficient way to prepare extremely long T-rich DNA nanowires for CuNCs synthesis. Based on this, our electrochemical strategy can realize label-free, turn-on detection of TdT activity via DNA-CuNCs generation. This electrochemical biosensor is highly sensitive and

selective, and displays good feasibility for TdT inhibitor screening. Moreover, our proposed TdT-mediated strategy is also applicable to a universal biosensing system for electrochemical turn-on detection of BamHI activity. The novel strategy presents a convenient and simple electrochemical method for DNA-related enzyme activity detection, which is helpful for further development of a miniaturized and low-cost electrochemical sensing platform for DNA-related enzyme-targeted biochemical investigation and drug discovery.

Experimental

Materials and apparatus

All chemicals were of analytical grade without further purification. Terminal deoxynucleotidyl transferase (TdT), 5× reaction buffer for TdT [1 M potassium cacodylate, 0.125 M Tris, 0.05% (v/v) Triton X-100, 5 mM $CoCl_2$ (pH 7.2)], DNA (involving single-stranded DNA, and hairpin DNA, their sequences are displayed in the Electronic Supplementary Material, ESM), and deoxythymidine triphosphate (dTTP) were obtained from Shanghai Sangon Biotechnology Co. Ltd. (Shanghai, China). H_2O_2 (30 wt%), 3-(N-morpholino) propanesulfonic acid (MOPS), copper sulfate, sodium ascorbate, $Na_4P_2O_7{\cdot}10H_2O$ (PP) were purchased from Sinopharm Chemical Reagent Co. Ltd (China). Graphite powder (99.99995%, 325 mesh) was purchased from Alfa Aesar and used for the preparation of graphene oxide (GO). Horseradish peroxidase (HRP), glucose oxidase (GO_X), alkaline phosphatase (ALP), acetyl cholinesterase (AChE), and papain were obtained from the Aladdin Industrial Co. BamHI, EcoRI, HindIII, Nb.BbvCl, and ExoIII were purchased from Sigma-Aldrich. The water used in the entire experiment was deionized water (18.25 MΩ cm) purified by a Millipore Milli-Q system.

All electrochemical experiments were performed with a CHI 660E electrochemical workstation (Shanghai Chenhua Instrument Co., China) and a conventional three-electrode system, where the modified glassy carbon electrode (3 mm in diameter), Ag/AgCl, and platinum wire acted as the work electrode, reference electrode, and counter electrode, respectively. A fluorescence spectrum was collected on a Hitachi F-4600 spectrometer (Hitachi Co. Ltd., Japan) under a voltage of 700 V with excitation and emission slit widths of 10 and 10 nm, respectively. Polyacrylamide gel electrophoresis (PAGE) was scanned by a ChemiDoc MP System, Bio-Rad, USA. The morphology of CuNCs was characterized by Philips CM200 UT transmission electron microscopy (TEM).

Preparation of TdT-yielded DNA-CuNCs

Preparation of grown T-rich DNA nanowires

Grown DNA nanowires were prepared with the polymerization solution containing single-stranded DNA (2 μM, 2.5 μL), dTTP (2 mM, 0.5 μL), TdT (5 U/μL, 0.1 μL), 5× reaction buffer for TdT (1 μL), and double-distilled water (0.9 μL). Then, the mixture was incubated at 37 °C for 2 h. To inactivate the enzyme, the polymerization solution was transferred into a thermostatic bath and kept at 75 °C for 10 min. The solution was stored at 4 °C before use.

Synthesis of grown DNA nanowires-templated copper nanoclusters (DNA-CuNCs)

A 5 μL volume of MOPS buffer (10 mM MOPS, 150 mM NaCl, pH 7.6) and ascorbic acid (2 mM, 10 μL) was added to the grown DNA nanowires solution above. The obtained mixture was sonicated for 2 min, in which $CuSO_4$ (1 mM, 10 μL) was added. Next, the resulting solution was incubated for 5 min at room temperature to form DNA-CuNCs.

Fabrication of the DNA-CuNCs/GO/GCE

GCE

Before modification, the glassy carbon electrode (GCE, 3 mm diameter) was polished with 1.0, 0.3, and 0.05 μm alumina slurry, respectively, and successively washed with double-distilled water, ethanol, and double-distilled water in an ultrasonic bath sequentially, and then dried under N_2 flow.

GO/GCE

The GCE was electrodeposited with graphene oxide (GO) suspension (1.0 mg/mL) by cyclic voltammetry from –1.5 to +0.5 V with a scanning rate of 10 mV/s under stirring for 10 cycles. The modified electrode was then thoroughly rinsed with double-distilled water to remove the physically adsorbed GO.

DNA-CuNCs/GO/GCE

Ten μL of the prepared DNA-CuNCs solution above was dropped onto the surface of GO/GCE to obtain DNA-CuNCs/GO/GCE. The prepared electrode was rinsed completely with phosphate buffer (0.1 M, pH 7.4). After incubation for 15 min, electrochemical measurements for TdT or BamHI activity detection was carried out for the prepared

DNA-CuNCs/GO/GCE. The modified electrode was stored at 4 °C in PBS (0.1 M, pH 7.4) when not in use.

The assay of TdT activity and its inhibitor

The 2.5 μL volume of ssDNA (2 μM) was added to PCR tube followed by the addition of dTTP (2 mM, 0.5 μL) and 5× reaction buffer for TdT (1 μL). Subsequently, different concentrations of TdT were added to the resulting solution and a final volume of 5 μL was obained. After 2 h at 37 °C, the synthesized TdT-mediated T-rich DNA nanowires were employed for the synthetic templates of DNA-CuNCs by the reduction of ascorbic acid. The entire conditions on preparation of DNA-CuNCs and fabrication of DNA-CuNCs/GO/GCE were confirmed as described above. Finally, the cyclic voltammograms of the resulting solutions were measured in PBS (0.1 M, pH 7.4) containing 5 mM H_2O_2.

For inhibitor assay, 0.1 μL of TdT (5 U/μL) was mixed with a series of different concentrations of sodium pyrophosphate (PP) and incubated for 5 min at 37 °C. Then ssDNA (2 μM, 2.5 μL), dTTP (2 mM, 0.5 μL), and 5× reaction buffer for TdT (1 μL) were added to the pre-prepared solution above and kept a total volume of 5 μL. The reaction conditions and subsequent steps were the same as those of TdT activity detection.

Detection of BamHI activity

To prepare the BamHI-relevant reaction solution, 2.4 μL of 10 μM DNA-Bam was mixed with different concentrations of BamHI and then 1 μL 10× BamHI reaction buffer was added and incubated at 37 °C for 2 h. Next, to inactivate BamHI, the total solution was left at 85 °C for 20 min.

After complete cleavage reaction, dTTP (2 mM, 0.5 μL), TdT (5 U/μL, 0.1 μL), 5× reaction buffer for TdT (1 μL), and double-distilled water (0.9 μL) were added to the Bam-mixture above (2.5 μL). Thereafter, the subsequent procedures were the same as those mentioned above.

Results and discussions

Principle and feasibility of the assay

A brief description of our electrochemical biosensing strategy for TdT activity detection based on grown DNA nanowires-templated copper nanoclusters (DNA-CuNCs) is shown in Scheme 1. The analysis is a three-step process: First, the key of our strategy is the exploitation of TdT to generate T-rich DNA sequence; there is a stronger specific interaction between copper ions and thymine than the other three bases. In the presence of dTTP, TdT catalyzes the continual polymerization of dTTP to elongate the 3′-OH terminal of DNA primers, thus bringing about long T-rich DNA nanowires. Second, the resulting grown DNA nanowires can be used as an efficient template for the formation of DNA-CuNCs. These unique DNA-CuNCs have high affinity with GO through noncovalent π–π stacking interaction. Third, on the basis of this mechanism, an electrochemical assay is established by self-assembling DNA-CuNCs onto a GO-modified glassy carbon electrode (GO/GCE) surface; this can electrocatalyze the reduction of H_2O_2, producing a strong electrochemical signal proportional to the amount of TdT. Consequently, the highly sensitive TdT activity assay can be realized by monitoring the change of the electrochemical signal. Therefore, the as-proposed label-free electrochemical strategy based on DNA-CuNCs is a promising candidate for highly sensitive detection of the activity of TdT and screening its inhibitor. What is interesting is that when the solution of DNA-Bam is mixed with BamHI, a new 3′-OH terminal is exposed due to the digestion of a phosphate group. Inspired by these phenomena, the proposed sensor can be used for the detection of BamHI activity by exploiting TdT-mediated extension. Conversely, DNA-CuNCs are not able to generate in the absence of BamHI. So, the prepared versatile electrochemical sensor provides a good prospect for a broader and general application in DNA-related enzyme-based biochemical studies, disease diagnosis, and drug discovery.

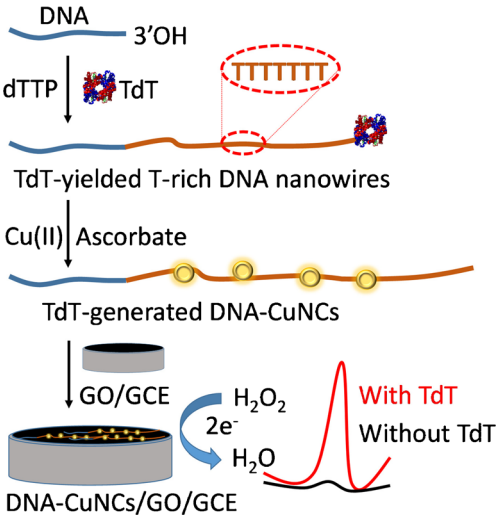

Scheme 1 Schematic illustration of the design and principle for electrochemical detection of TdT activity by using grown DNA nanowires-templated copper nanoclusters (DNA-CuNCs)

Characterization of TdT-yielded DNA-CuNCs

According to the previous reports, it is known that the solution of DNA-CuNCs exhibits strong fluorescence [21, 43, 44]. To evaluate the feasibility of our grown DNA nanowires-templated CuNCs strategy, we chose a random ssDNA as the primer for TdT polymerization, in which process the short ssDNA primer can be converted to a long T-rich DNA

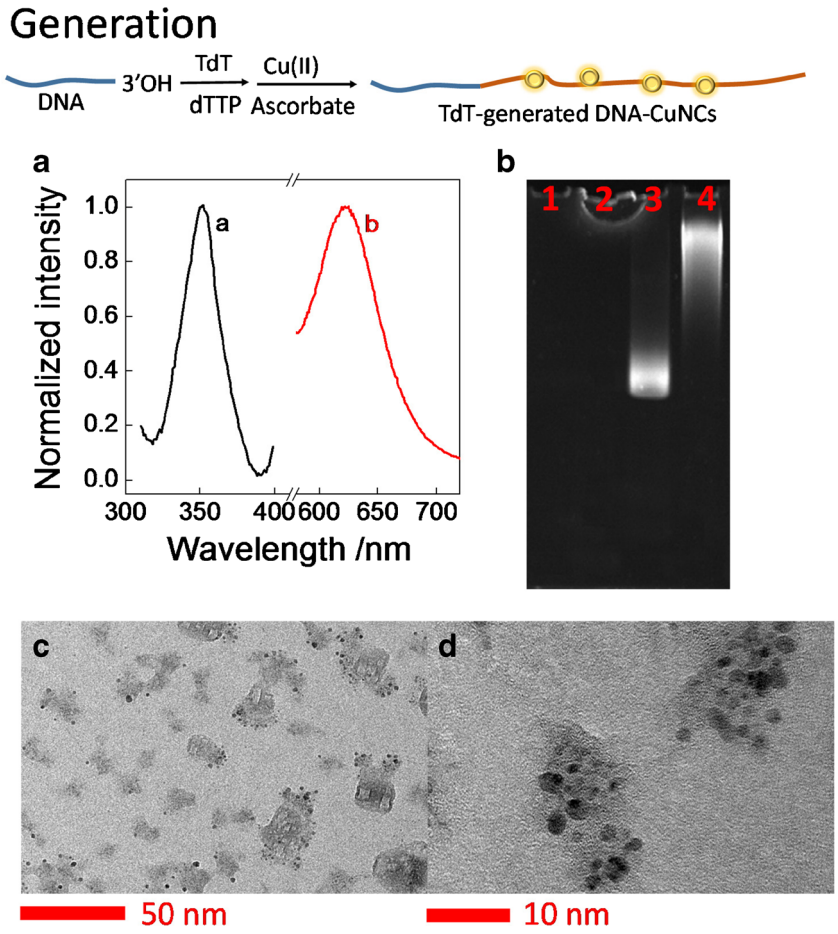

Fig. 1 **(A)** Excitation (curve a) and emission (curve b) normalized intensity of fluorescence spectra of as-prepared TdT-generated DNA-CuNCs; **(B)** PAGE analysis of sole TdT (lane 1), sole dTTP (lane 2), sole ssDNA (lane 3), and TdT-extended poly-T DNA (lane 4); **(C)** and **(D)** TEM images of DNA-CuNCs with different magnifications. [TdT] = 100 U/mL, [dTTP] = 0.2 mM, [ssDNA] =1 μM

nanowire to support the formation of DNA-CuNCs. The obtained DNA-CuNCs exhibit an excitation peak centered at 350 nm and an emission peak centered at 620 nm (Fig. 1A). The results are similar to those obtained by the Yao group [21], and also demonstrate that DNA-CuNCs have been successfully synthesized. Moreover, fluorescence responses of the different samples are also displayed in Supplementary Fig. S1 (see ESM). It was shown that a strong fluorescence emission of TdT-generated DNA-CuNCs at 620 nm was detected, but no obvious fluorescence signal was obtained in the absence of TdT, DNA, dTTP, or Cu(II), respectively. To evaluate further the TdT-generated T-rich DNA nanowires, 8% PAGE was performed to analyze the polymerization product. Obviously, as shown in Fig. 1B, ssDNA (lane 3) and TdT-generated T-rich DNA nanowires (lane 4) can be identified clearly by the migration position in gel, and there are no bands on just TdT (lane 1) or dTTP (lane 2), indicating the feasibility of the proposed assay.

Generally, poly-T DNAs with different lengths were executed for the formation of fluorescent DNA-CuNCs. As depicted in Supplementary Fig. S2, when TdT-generated T-rich DNA nanowires acted as a synthetic template of DNA-CuNCs, they emitted stronger fluorescence than other samples involving purchased T40 at varying concentrations. It may be caused by the following two reasons: (1) the longer poly-T DNA, the better the protection effect by repelling the polar solvent from the surface of the DNA-CuNCs, thus enhancing the fluorescence intensity [45]; (2) the optical properties of DNA-CuNCs were improved due to fluorescence resonance energy transfer (FRET) similar to the reported FRET-based interaction among gold nanoclusters [46]. Meanwhile, we found that the fluorescence intensity increased at first, then began to decrease at 5 μM T40, suggesting the number of T bases can affect the formation of DNA-CuNCs. The reason for this is that when the T40 concentration was less than 5 μM, Cu(II) attached in T40 may be sufficient, leading to an increasing trend. Conversely, indigent Cu(II) is not enough for extra T40, resulting in a fluorescence decrease. These results revealed that TdT-generating poly-T DNA nanowire has a brighter outlook than short-chain poly-T DNA for the preparation of DNA-CuNCs. Moreover, our proposed DNA-CuNCs showed high fluorescence and good repeatability (Supplementary Fig. S3), presenting a great potential in biosensing. Afterwards, transmission electron microscopy (TEM) images of DNA-CuNCs were recorded and revealed that the as-prepared DNA-CuNCs were ultra-small with a size

of approximately 3 nm, and were arranged in clusters (Fig. 1C and D); it depended on the template role of TdT-generated T-rich DNA nanowires.

Electrochemical behaviors of the sensor

The stepwise modification process of the biosensor and the adsorption interaction of DNA-CuNCs and GO were verified by electrochemical measurements. Figure 2A displays the CV curves of the modified electrodes at different fabrication steps in 5 mM $[Fe(CN)_6]^{3-/4-}$ containing 0.1 M KCl. Compared with the bare GCE, the peak current of GO-modified GCE increased owing to the excellent conductivity of GO. When the electrode was modified with our DNA-CuNCs, decreased peak currents and poor reversibility were found due to the insulating effect of DNA. With DNA-CuNCs assembled on the GCE directly, the peak currents are equal to that at GCE; this is attributed to the fact that DNA-CuNCs cannot be adsorbed without GO. The assembly process of the sensor was also tested with electrochemical impedance spectroscopy (EIS) method. As illustrated in Fig. 2B, the results of EIS data are in accordance with the CV data, confirming further the successful construction of the sensor and the adsorption interaction of DNA-CuNCs and GO. Generally, an electrode–electrolyte interface can be described as the equivalent electrical circuit in terms of a resistor and capacitor. The impedance spectra are fitted by a simple Randle circuit, as shown in the inset of Fig. 2B. Here, Rs and Rct represent ohmic resistance of electrolyte solution and the electron-transfer resistance of the redox, respectively. Based on the theoretical model, a nice agreement in terms of the magnitude and phase angle of impedance over the frequency range from 0.1 Hz to 100 kHz were achieved between the simulation and experimental results obtained on the modified electrode. The fitting values for the stepwise assembled layers on the electrode of electrochemical impedance spectroscopy are presented in Supplementary Table S1.

It is intriguing for us to explore the electrocatalytic property of our proposed DNA-CuNCs, which is scarce. Moreover, the formation of T-rich DNA nanowires depends on the polymerization of TdT, so probing the TdT activity can be achieved by a signal-on electrochemical response of DNA-CuNCs. It can be seen that no current response was observed in the absence of TdT (Fig. 2C), and what is more, when DNA-CuNCs were introduced, an outstanding reduction peak at –0.5 V was observed on the presence of TdT. Furthermore, in DNA-CuNCs preparation process, sole TdT, sole dTTP, sole Cu(II), or DNA (Supplementary Fig. S4A) leads to

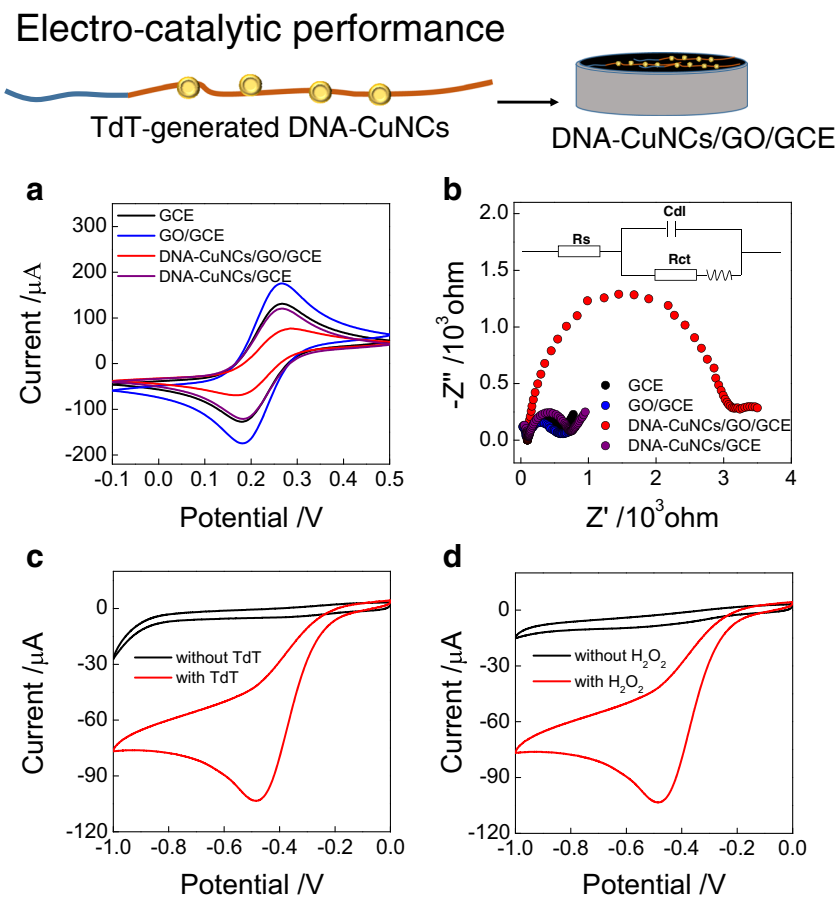

Fig. 2 **(A)** Cyclic voltammograms (CV) and **(B)** electrochemical impedance spectroscopy (EIS) of the bare GCE, GO/GCE, DNA-CuNCs/GO/GCE, and DNA-CuNCs/GCE in 5 mM $[Fe(CN)_6]^{3-/4-}$ containing 0.1 M KCl, the insert is the equivalent circuit for the EIS data; **(C)** electrochemical detection of TdT activity based on TdT-generated DNA-CuNCs in PBS (0.1 M, pH 7.4) containing 5 mM H_2O_2; **(D)** cyclic voltammograms of DNA-CuNCs/GO/GCE in the presence or absence of 5 mM H_2O_2. [TdT] = 100 U/mL, [dTTP] = 0.2 mM, [ssDNA] =1 μM

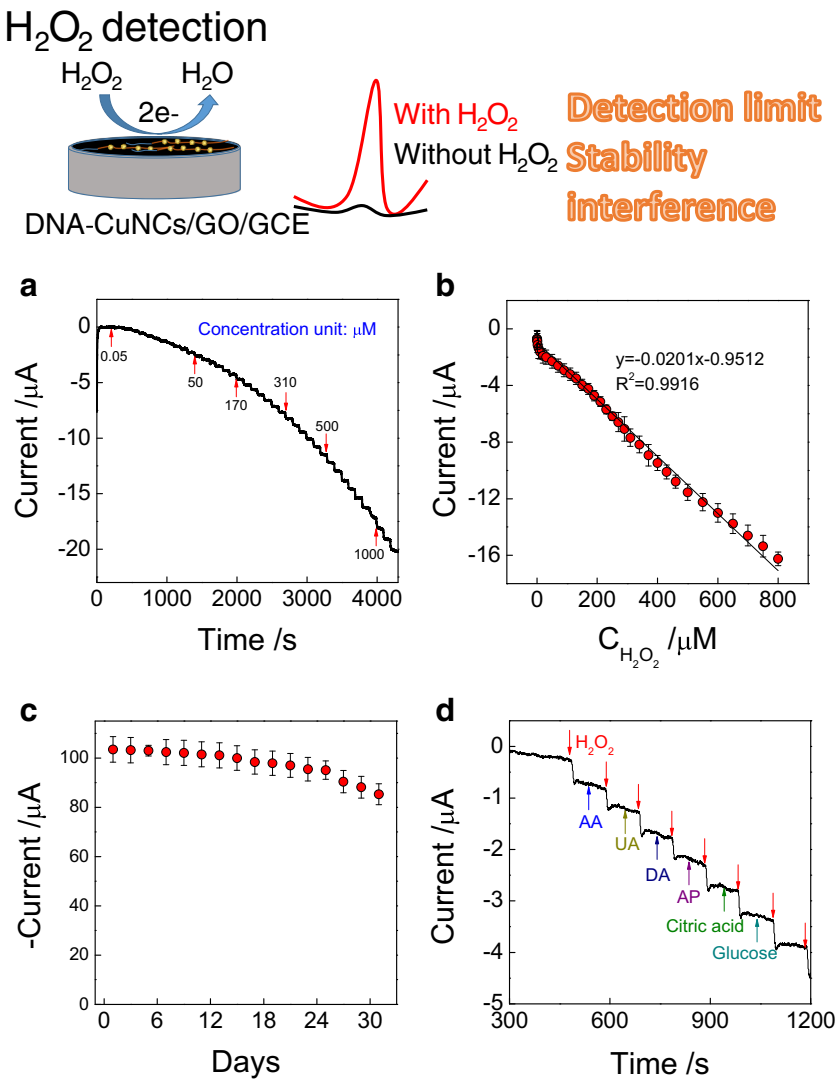

Fig. 3 **(A)** Current-time response obtained in 0.1 M PBS by increasing different concentrations of H_2O_2 on the DNA-CuNCs/GO/GCE at –0.3 V; **(B)** the plot of response current versus the concentration of H_2O_2; **(C)** stability test on the DNA-CuNCs/GO/GCE within one month; **(D)** amperometric i-t response at DNA-CuNCs/GO/GCE for the successive addition of 0.1 mM H_2O_2, but alternation of 1 mM AA, UA, DA, AP, citric acid or glucose solution

negligible electrochemical signal. The same phenomenon was also observed with lack of one of the other reaction compositions (involving TdT, dTTP, Cu(II), or DNA) (Supplementary Fig. S4B), foreshadowing TdT activity detection. Later on, we further tried to assess the electrocatalytic property of DNA-CuNCs, and found that the proposed sensor exhibits an excellent electrochemical signal in PBS (0.1 M, pH 7.4) with 5 mM H_2O_2 rather than without H_2O_2 (Fig. 2D), indicating good electrochemical performance of DNA-CuNCs for the construction of TdT-based biosensor.

Analytical performance test of the proposed biosensor

The present strategy is based on TdT-mediated extension and the formation of DNA-CuNCs. Some experimental parameters, which greatly influence the sensitivity of the sensor, have been optimized. Supplementary Figure S5A exhibits that the response current upon H_2O_2 reduction increases with the increasing TdT-mediated extension time and then approaches a constant value at 2 h. Thus, 2 h of extension time was selected in the following experiments. The effect of adsorption time on DNA-CuNCs and GO/GCE ranged from 0 to 60 min, as can be seen from Supplementary Fig. S5B, the current intensity gradually increased with the increasing absorption time until 15 min, and the absorption time longer than 15 min did not produce further signal change. Thus, 15 min of adsorption time was chosen. A further study was performed to investigate the influence of pH (Supplementary Fig. S5C), and the maximal reduction peak current of H_2O_2 was obtained at pH 7.4; a buffer solution (pH 7.4) was selected as the supporting electrolyte in the experiments. Additionally, as noted in Supplementary Fig. S5D, the current intensity increased with increasing dTTP concentration without changing other reaction conditions. This is because the more dTTP, the longer DNA nanowires, which then result in the stronger electrochemical signal. When the concentration of dTTP is 2 mM, the current gradually reaches a plateau. So, 2 mM of dTTP was chosen for the optimal reaction concentration.

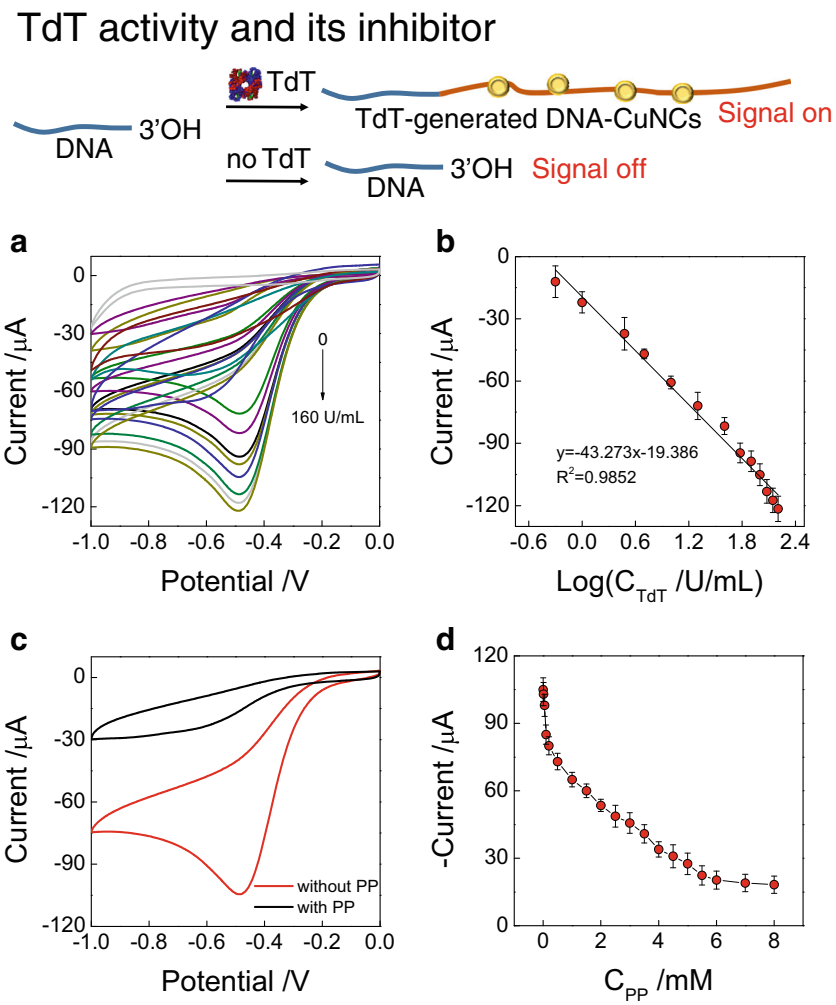

Fig. 4 **(A)** Cyclic voltammograms employed by probing TdT activity with various final concentrations (0, 0.5, 1, 3, 5, 10, 20, 40, 60, 80, 100, 120, 140, and 160 U/mL) based on our synthesis strategy for DNA-CuNCs; **(B)** linear relationship between peak currents and the logarithm of the TdT concentrations; **(C)** electrochemical signal change in the presence or absence of 8 mM sodium pyrophosphate (PP); **(D)** various final concentrations (0, 0.01, 0.05, 0.1, 0.2, 0.5, 1, 1.5, 2, 2.5, 3, 3.5, 4, 4.5, 5, 5.5, 6, 7, and 8 mM) of PP were used for investigation of TdT inhibition

To convince large current density and avert the interference from other biologically active molecules, the amperometric current-time response of the DNA-CuNCs/GO/GCE with successive addition of varying concentrations of H_2O_2 in 0.1 M PBS solution (pH 7.4) was tested, and the results are presented in Fig. 3A and Supplementary Fig. S6. The DNA-CuNCs-based biosensor presents quick response with the introduction and change of H_2O_2 concentration. Moreover, as noted in Fig. 3B, the current response of the sensor is proportional to H_2O_2 concentration in the range of 0.05 to 1000 μM. The limit of detection was experimentally found to be 0.01 μM ($S/N = 3$), which is lower than those of most of previously reported H_2O_2 assays (Supplementary Table S2). Therefore, DNA-CuNCs is an ideal electrochemical sensing material for H_2O_2 detection with high sensitivity.

To attempt receiving an outstanding signal in the presence of traces H_2O_2 by amperometric i-t curves, the proposed sensor had to meet two criteria: long-time operation and excellent stability. When the sensor was not in use, it was stored at 4 °C in PBS (0.1 M, pH 7.4). The stability of the designed biosensor was also evaluated by measuring its current responses at 4-wk-period storage. The current responses had no obvious change after storage for 3 wk, only in the fourth wk there was a little decline, showing good stability and detection reliability (Fig. 3C). Then, the effect on some interfering electroactive species, including ascorbic acid (AA), uric acid (UA), dopamine (DA), acetaminophen (AP), citric acid, or glucose, for the current response was evaluated at the potential of –0.3 V (Fig. 3D). We can observe a significant change of current with the addition of 0.1 mM H_2O_2, while the currents of the interfering substances are nearly the same as that in the blank solution. The results reveal that the prepared biosensor presents a new insight into H_2O_2-relevant determination in biological fluids without any interference.

Probing TdT activity and its inhibitor

The proposed DNA-CuNCs and their electrocatalytic property were further employed for probing TdT activity. As far as we know, altered expression levels and activity of TdT play an important role for cancer development and might deteriorate the response to anticancer chemotherapy. In our research,

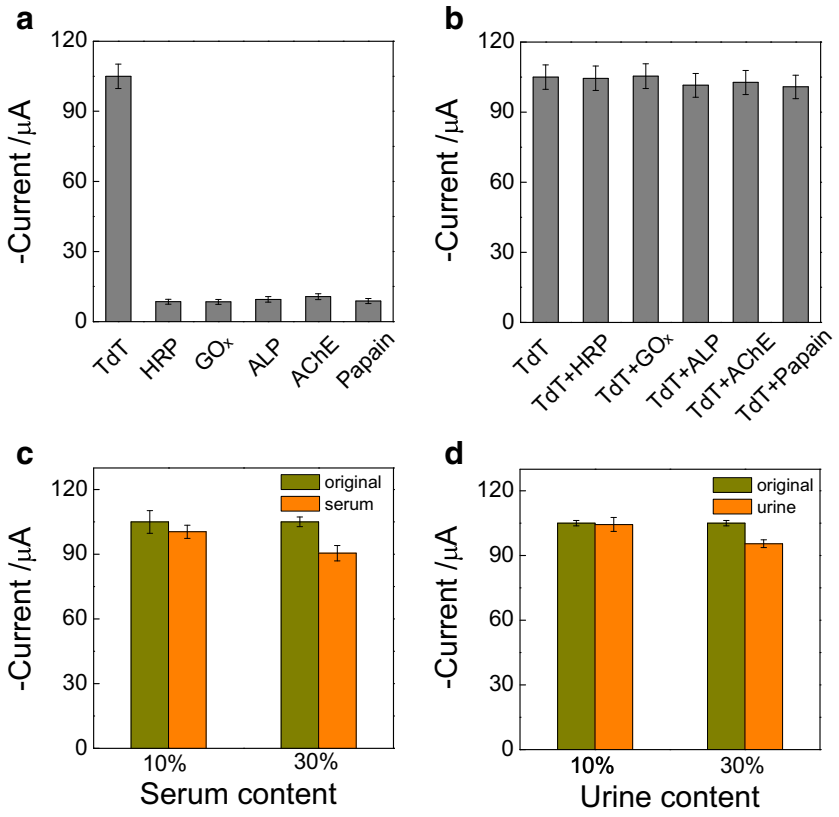

Fig. 5 **(A)** Selectivity of the proposed sensor for TdT over other biomolecules including HRP, GO_X, ALP, AChE, or Papain, respectively; **(B)** interference in the presence of TdT, together with HRP, GO_X, ALP, AChE, or Papain, respectively; TdT activity assay in different volume ratios of biological fluids, such as **(C)** serum and **(D)** urine, original: namely the TdT activity assay without serum or urine. The concentrations of all objects are 100 U/mL

randomly arrayed T-rich DNA nanowires are received by TdT-mediated extension from the 3′-OH terminus of ssDNA, which can be performed for the template of DNA-CuNCs. Consequently, TdT activity can be facilely probed by the change of electrochemical response. As shown in Fig. 4A, an obvious response current peak of H_2O_2 near –0.5 V appears and the electrochemical response currents of DNA-CuNCs/GO/GCE increase gradually with the increment of concentrations of TdT. Meanwhile, Fig. 4B shows a line correction between the electrochemical current and the logarithms of TdT concentrations, ranging from 0.5 to 160 U/mL. According to the $S/N = 3$ rule, the detection limit of TdT was calculated to be 0.1 U/mL, which is lower than those of most of previously reported TdT assays (SupplementaryTable S3). Thus, a novel, simple, and label-free electrochemical strategy for TdT activity detection was developed based on unique electrocatalytic property of our proposed DNA-CuNCs.

For demonstrating the possible application of the proposed system to screen the potential enzyme inhibitor, $Na_4P_2O_7$ (PP), a potent small molecule inhibitor of the TdT [21] was chosen as model. As exposed in Fig. 4C, the electrochemical signal of the system in the presence of PP was nearly the same as that of the blank solution, but a strong electrochemical reduction response was observed without PP. The results indicated that PP is an effective inhibitor for TdT. Additionally, different concentrations of PP were added to the sensing system, and the data are summarized in Fig. 4D. The electrochemical responses of the sensing system decreased gradually with the enhancement of the PP concentrations. The IC_{50} value (half maximal inhibitory concentration of the inhibitor) is determined to be about 1.5 mM, which is agreeable with the literature values [21]. Thus, these results clearly suggest that the proposed assay has a considerable potential to qualitatively screen TdT inhibitors and provide a broad prospect for TdT-based drug discovery.

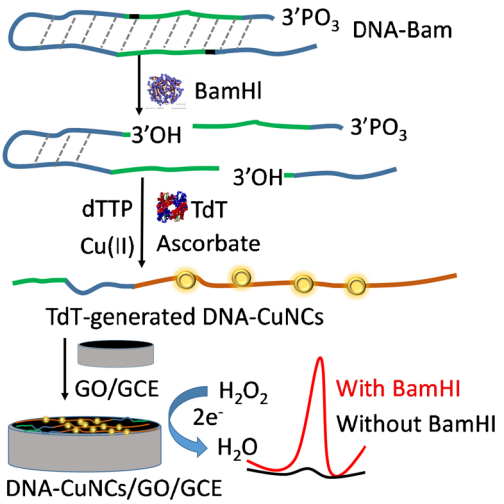

Scheme 2 Schematic representation of BamHI activity assay principle based on the TdT-generated DNA-CuNCs synthesis

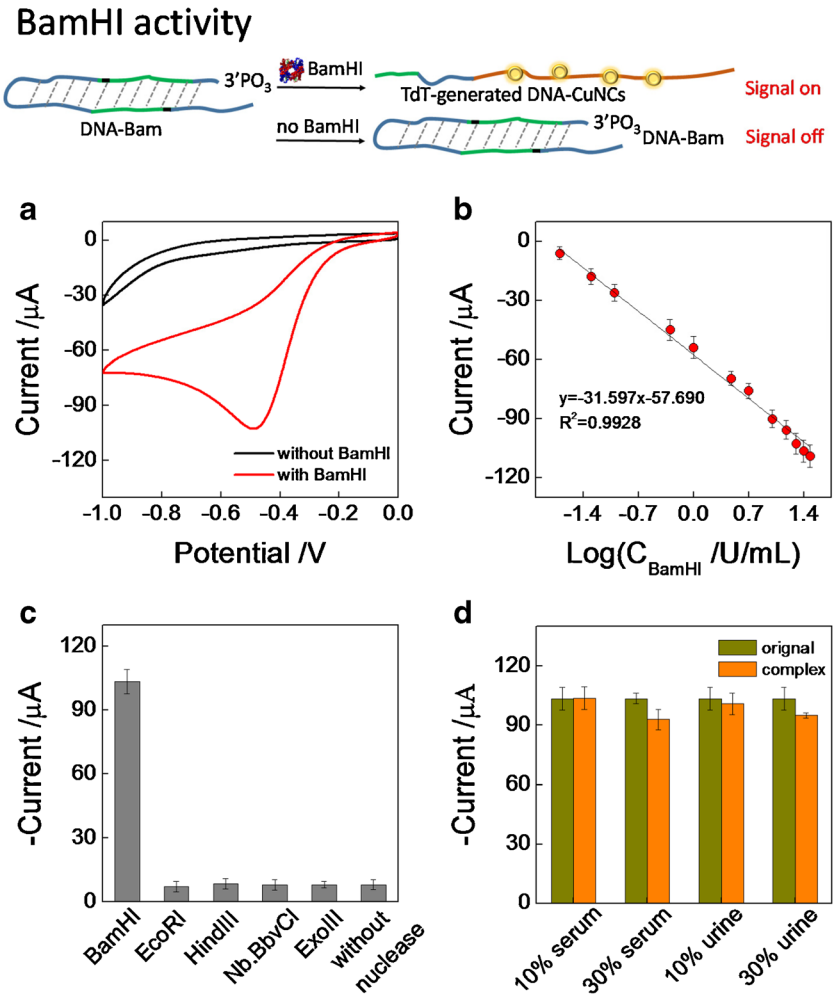

Fig. 6 **(A)** Electrochemical responses of BamHI activity based on TdT-generated DNA-CuNCs in the presence or absence of 20 U/mL BamHI; **(B)** calibration curve of this BamHI-based sensor with the increase of different final concentrations of BamHI (0.02, 0.05, 0.1, 0.5, 1, 3, 5, 10, 15, 20, 25, 30 U/mL); **(C)** selectivity of the developed biosensor, the concentrations of all objects are 20 U/mL; **(D)** comparison of the BamHI detection assay in original sample (namely the reaction solution without serum/urine) and serum/urine samples

Selectivity and interference are the key factors to assess the sensing performance of the proposed sensor, especially for the potential applications in practical biological samples, because the physiological environment is complex. To investigate the specificity of the sensor for TdT, the response to different interfering species containing HRP, GO_X, ALP, AChE, and papain was studied. As shown in Fig. 5A, compared with other interfering molecules, the electrochemical response of the sensor has a greater enhancement toward TdT. Furthermore, anti-interference was subsequently evaluated and illustrated by adding other interfering molecules to the TdT-based reaction solution, and negligible change of electrochemical signals was observed (Fig. 5B). Therefore, the proposed sensor exhibited excellent selectivity toward TdT and could be applied to detecting TdT activity in living cells and tissue.

In order to assess the practicality of the sensor, we performed the analysis of TdT in real biological systems. To eliminate the interference from reducing substance, a TdT-trapping test was performed in diluted serum or urine samples spiked with different concentrations of TdT. The current response in 10% serum or urine sample is basically no change, while there is a sight change in 30% serum or urine sample (Fig. 5C and D). The results confirmed that the proposed method was feasible to detect TdT in real biological samples. To further evaluate the applicability of this proposed TdT sensor for detection in real samples, recovery measurement of TdT spiked in 10% serum or urine (v/v) was conducted by the proposed electrochemical approach. As shown in Supplementary Table S4, the recoveries were in an acceptable range, from 94.0% to 103.0% for serum samples and from 95.0% to 107.0% for urine samples; the RSD were in the range from 1.7% to 5.1% for serum samples and from 1.1% to 4.5% for urine samples, indicating an acceptable accuracy.

Versatile platform for BamHI activity detection

As a site-specific endonuclease, BamHI endonuclease can be used to detect the hepatitis C virus (HCV), presenting a great biological significance [30]. The working principle of the designed electrochemical method for probing the BamHI activity is schematically shown in Scheme 2. As is well-known, native BamHI restriction enzyme recognizes G^GATCC sites for

double digestion. When BamHI was introduced into DNA-Bam reaction system, DNA-Bam could be digested and a new 3′-OH was exposed. The resulting 3′-OH DNA was used for TdT-mediated extension and the ensuing experiments, obtaining a signal-on electrochemical signal, which can be carried out for the quantitative detection of BamHI activity (Fig. 6A). Conversely, in the absence of BamHI, the 3′-PO_3 passivated hairpin DNA probe failed to induce electrochemical signal. The electrochemical current at –0.5 V was systematically decreased and linear to log(C_{BamHI}) in the concentration range of 0.02 to 30 U/mL (Fig. 6B). The LOD based on $S/N = 3$ was estimated to be 0.004 U/mL, which is lower than that reported for most other assays listed in Supplementary Table S5.

The selectivity was also evaluated. Some other irrelevant enzymes, such as EcoRI, HindIII, Nb.BbvCI, and NdeI, were used as control. The results persuasively showed that none of these representative interferents, except BamHI, could evoke a conspicuous electrochemical signal (Fig. 6C). The practicability of this sensing platform was demonstrated by detecting BamHI in diluted serum or urine sample (10% or 30%). As shown in Fig. 6D, the proposed sensor exhibits excellent current response with 10% or 30% serum or urine, indicating the potential of this method for applications of detecting BamHI activity in complicated real samples.

Conclusions

An electrochemical sensing platform for TdT with high sensitivity and selectivity was ingeniously designed and established by the catalytic capability of TdT-generated T-rich DNA nanowires-templated CuNCs. The proposal of DNA-CuNCs opens up a new window for TdT-based electrochemical sensor. The DNA-CuNCs were developed based on the template role of TdT-generated T-rich DNA nanowires. To our best knowledge, it is rare that the DNA-CuNCs are applied for electrochemical detection of TdT activity and its inhibitor screening. Moreover, DNA-CuNCs-based sensing strategy was also extended to the detection of different biomolecules, such as BamHI, which indicated the broad application of the developed DNA-CuNCs in biological analysis. This new biosensing strategy shows great promise for further development of CuNCs-based biosensors, such as for a molecular biology tool and for early clinical diagnosis or drug discovery.

Acknowledgements Financial support from the National Natural Science Foundation of China (41576098, 81273130 and 21605089), the Open Subject of State Key Laboratory of Chemo/Biosensing and Chemometrics (2016001), Project of Academic Research Foundation of Ningbo University (XYL17002), the Ningbo Municipal Natural Science Foundation (2016A610052), and the Science and Technology Department of Zhejiang Province of China (2016C33176, 2016R405068) are gratefully acknowledged. This work was also sponsored by K.C. Wong Magna Fund in Ningbo University.

Compliance with ethical standards

Conflict of interest The authors declare that they have no conflict of interest.

References

1. Kornberg A. Ten commandments: Lessons from the enzymology of DNA replication. J Bacteriol. 2000;182:3613–8.
2. Benkovic SJ, Valentine AM, Salinas F. Replisome-mediated DNA replication. Annu Rev Biochem. 2001;70:181–208.
3. Kunkel TA, Burgers PM. Dividing the workload at a eukaryotic replication fork. Trends Cell Biol. 2008;18:521–7.
4. Berdis AJ. Mechanisms of DNA polymerases. Chem Rev. 2009;109:2862–79.
5. Michaelis J, Treutlein B. Single-molecule studies of RNA polymerases. Chem Rev. 2013;113:8377–99.
6. David SS, Williams SD. Chemistry of glycosylases and endonucleases involved in base-excision repair. Chem Rev. 1998;98:1221–62.
7. Ikeda RA, Dervan PB. Sequence-selective inhibition of restriction endonucleases by the polyintercalator bis(methidium)spermine. J Am Chem Soc. 1982;104:296–7.
8. Bollum FJ. Thermal conversion of nonpriming deoxyribonucleic acid to primer. J Biol Inorg Chem. 1959;234:2733–4.
9. Bollum FJ. Chemically defined templates and initiators for deoxypolynucleotide synthesis. Science. 1964;144:560.
10. Baltimore D. Is terminal deoxynucleotidyl transferase a somatic mutagen in lymphocytes? Nature. 1974;248:409–11.
11. Benedict CL, Gilfillan S, Thai TH, Kearney JF. Terminal deoxynucleotidyl transferase and repertoire development. Immunol Rev. 2000;175:150–7.
12. Kunkel TA, Gopinathan KP, Dube DK, Snow ET, Loeb LA. Rearrangements of DNA mediated by terminal transferase. Proc Natl Acad Sci U S A. 1986;83:1867–71.
13. Kung PC, Long JC, McCaffrey RP, Ratliff RL, Harrison TA, Baltimore D. Terminal deoxynucleotidyl transferase in the diagnosis of leukemia and malignant lymphoma. Am J Med. 1978;64:788–94.
14. Stass SA, McGraw TP, Folds JD, Odle B, Bollum FJ. Terminal transferase in acute lymphoblast leukemia in remission. Am J Clin Pathol. 1981;75:838–40.
15. Venditti A, Del Poeta G, Buccisano F, Tamburini A, Aronica G, Bruno A, et al. Biological pattern of AML-M0 versus AML-M1: response. Blood. 1997;89:345–6.
16. Hutter JJ. Childhood leukemia. Pediatr Rev. 2010;31:234–41.
17. Hunger SP, Raetz EA, Loh ML, Mullighan CG. Improving outcomes for high-risk ALL: translating new discoveries into clinical care. Pediatr Blood Cancer. 2011;56:984–93.
18. Goldschneider I, Gregoire KE, Barton RW, Bollum FJ. Demonstration of terminal deoxynucleotidyl transferase in thymocytes by immunofluorescence. Proc Natl Acad Sci U S A. 1977;74:734–8.
19. Kung P, Gottlieb P, Baltimore D. Terminal deoxynucleotidyltransferase. Serological studies and radioimmunoassay. J Biol Chem. 1976;251:2399–404.
20. Liu ZL, Li W, Nie Z, Peng FF, Huang Y, Yao SZ. Randomly arrayed G-quadruplexes for label-free and real-time assay of enzyme activity. Chem Commun. 2014;50:6875–8.

21. Peng FF, Liu ZL, Li W, Huang Y, Nie Z, Yao SZ. Enzymatically generated long polyT-templated copper nanoparticles for versatile biosensing assay of DNA-related enzyme activity. Anal Methods. 2015;7:4355–61.
22. Yuan YJ, Li WH, Liu ZL, Nie Z, Huang Y, Yao SZ. A versatile biosensing system for DNA-related enzyme activity assay via the synthesis of silver nanoclusters using enzymatically-generated DNA as template. Biosens Bioelectron. 2014;61:321–7.
23. Hu YF, Shen QP, Li W, Liu ZL, Nie Z, Yao SZ. A TdT-mediated cascade signal amplification strategy based on dendritic DNA matrix for label-free multifunctional electrochemical biosensing. Biosens Bioelectron. 2015;63:331–8.
24. Al Minawi Z, Lee YF, Hakansson D, Johansson F, Lundin C, Saleh Gohari N, et al. The ERCC1/XPF endonuclease is required for completion of homologous recombination at DNA replication forks stalled by inter-strand cross-links. Nucleic Acids Res. 2009;37:6400–13.
25. Yeeles JTP, Dillingham MS. The processing of double-stranded DNA breaks for recombinational repair by helicase-nuclease complexes. DNA Repair. 2010;9:276–85.
26. Redondo P, Prieto J, Muñoz IG, Alibés A, Stricher F, Serrano L, et al. Molecular basis of *Xeroderma pigmentosum* group C DNA recognition by engineered meganucleases. Nature. 2008;456:107–11.
27. Gao YT, Han T, Li Y, Yang B, Wang YJ, Wang FM, et al. Enhanced specificity of real-time PCR for measurement of hepatitis B virus cccDNA using restriction endonuclease and plasmid-safe ATP-dependent DNase and selective primers. J Virol Methods. 2010;169:181–7.
28. Kanaras AG, Wang Z, Hussain I, Brust M, Cosstick R, Bates AD. Site-specific ligation of DNA-modified gold nanoparticles activated by the restriction enzyme styI. Small. 2007;3:67–70.
29. Pingoud A, Jeltsch A. Structure and function of type II restriction endonucleases. Nucleic Acids Res. 2001;29:3705–27.
30. Tang DP, Tang J, Su BL, Li QF, Chen GN. Electrochemical detection of hepatitis C virus with signal amplification using *Bam*HI endonuclease and horseradish peroxidase-encapsulated nanogold hollow spheres. Chem Commun. 2011;47:9477–9.
31. Ma L, Su M, Li T, Wang ZX. Microarray-based fluorescence assay of endonuclease functionality and inhibition. Analyst. 2013;138:1048–52.
32. Molard Y. Clustomesogens: liquid crystalline hybrid nanomaterials containing functional metal nanoclusters. Acc Chem Res. 2016;49:1514–23.
33. Jin S, Wang SX, Xiong L, Zhou M, Chen S, Du WJ, et al. Two electron reduction: from quantum dots to metal nanoclusters. Chem Mater. 2016;28:7905–11.
34. Jin RC, Zeng CJ, Zhou M, Chen YX. Atomically precise colloidal metal nanoclusters and nanoparticles: fundamentals and opportunities. Chem Rev. 2016;116:10346–413.
35. Zheng KY, Setyawati MI, Lim TP, Leong DT, Xie JP. Antimicrobial cluster bombs: silver nanoclusters packed with daptomycin. ACS Nano. 2016;10:7934–42.
36. Goswami N, Yao QF, Luo ZT, Li JG, Chen TK, Xie JP. Luminescent metal nanoclusters with aggregation-induced emission. J Phys Chem Lett. 2016;7:962–75.
37. Porta M, Nguyen MT, Tokunaga T, Ishida Y, Liu WR, Yonezawa T. Matrix sputtering into liquid mercaptan: from blue-emitting copper nanoclusters to red-emitting copper sulfide nanoclusters. Langmuir. 2016;32:12159–65.
38. Yau SH, Varnavski O, Goodson T III. An ultrafast look at Au nanoclusters. Acc Chem Res. 2013;46:1506–16.
39. Wang TY, Wang DC, Padelford JW, Jiang J, Wang GL. Near-infrared electrogenerated chemiluminescence from aqueous soluble lipoic acid Au nanoclusters. J Am Chem Soc. 2016;138:6380–3.
40. Gieseking RL, Ratner MA, Schatz GC. Semi-empirical modeling of Ag nanoclusters: new parameters for optical property studies enable determination of double excitation contributions to plasmonic excitation. J Phys Chem A. 2016;120:4542–349.
41. Wang Z, Si L, Bao J, Dai Z. A reusable microRNA sensor based on the electrocatalytic property of heteroduplex-templated copper nanoclusters. Chem Commun. 2015;51:6305–7.
42. Qing Z, He X, Qing T, Wang K, Shi H, He D, et al. Poly(thymine)-templated fluorescent copper nanoparticles for ultrasensitive label-free nuclease assay and its inhibitors screening. Anal Chem. 2013;85:12138–43.
43. Su XX, Liu JB. pH-guided self-assembly of copper nanoclusters with aggregation-induced emission. ACS Appl Mater Interfaces. 2017;9:3902–10.
44. Jia XF, Li J, Han L, Ren JT, Yang X, Wang EK. DNA-hosted copper nanoclusters for fluorescent identification of single nucleotide polymorphisms. ACS Nano. 2012;6:3311–7.
45. Shang L, Brandholt S, Stockmar F, Trouillet V, Bruns M, Nienhaus GU. Effect of protein adsorption on the fluorescence of ultra-small gold nanoclusters. Small. 2012;8:661–5.
46. Sun CJ, Yang H, Yuan Y, Tian X, Wang LM, Guo Y, et al. Controlling assembly of paired gold clusters within apoferritin nanoreactor for in vivo kidney targeting and biomedical imaging. J Am Chem Soc. 2011;133:8617–724.